Eur. Phys. J. C 51, 713–719 (2007)
DOI 10.1140/epjc/s10052-007-0294-7

THE EUROPEAN PHYSICAL JOURNAL C

Regular Article – Theoretical Physics

Virtual effects of split-SUSY in Higgs productions at linear colliders

Fei Wang[1], Wenyu Wang[2], Fuqiang Xu[2], Jin Min Yang[3,2,a], Huanjun Zhang[2,4]

[1] Center for High Energy Physics, Tsinghua University, Beijing 100084, P.R. China
[2] Institute of Theoretical Physics, Academia Sinica, Beijing 100080, P.R. China
[3] CCAST (World Laboratory), P.O. Box 8730, Beijing 100080, P.R. China
[4] Department of Physics, Henan Normal University, Xinxiang 453007, P.R. China

Received: 27 December 2006 / Revised version: 21 February 2007 /
Published online: 22 May 2007 –

Abstract. In split supersymmetry, gauginos and higgsinos are the only supersymmetric particles possibly accessible at foreseeable colliders like the CERN Large Hadron Collider (LHC) and the International Linear Collider (ILC). In order to account for the cosmic dark matter measured by WMAP, these gauginos and higgsinos are stringently constrained and could be explored at the colliders through their direct productions and/or virtual effects in some processes. The clean environment and high luminosity of the ILC render the virtual effects at percent level meaningful in unraveling the new physics effects. In this work we assume split supersymmetry and calculate the virtual effects of the WMAP-allowed gauginos and higgsinos in the Higgs productions $e^+e^- \to Zh$ and $e^+e^- \to \nu_e\bar{\nu}_e h$ through WW fusion at the ILC. We find that the production cross section of $e^+e^- \to Zh$ can be altered by a few percent in some part of the WMAP-allowed parameter space, while the correction to the WW fusion process $e^+e^- \to \nu_e\bar{\nu}_e h$ is below 1%. Such virtual effects are correlated with the cross sections of chargino pair productions and can offer complementary information in probing split supersymmetry at the colliders.

PACS. 14.80.Ly; 95.35.+d

1 Introduction

Since supersymmetry (SUSY) is so appealing in particle physics, cosmology and string theory, its exploration will be a central focus of future collider experiments. If SUSY is at the TeV scale, as required by solving the fine-tuning problem in particle physics, the LHC expects to discover it or at least reveal some of its fingerprints, and then the ILC [1–3] will zoom in on its precision test and map out its detailed structure. However, if fine-tuning in particle physics works in nature just like the fine-tuning for the cosmological constant, SUSY may turn out to be a kind of split-SUSY [4–6], in which all scalar supersymmetric particles (sfermions and additional Higgs bosons) are superheavy and only gauginos and higgsinos are possibly light and accessible at foreseeable colliders like the LHC and ILC. So, if split-SUSY is the true story, the focus of experimental and theoretical studies on SUSY will be concerned with gauginos and higgsinos.

To facilitate the collider searches for gauginos and higgsinos in split-SUSY, it is important to examine the possible range of their masses by considering various direct and indirect constraints and requirements. The lightness of the gauginos and higgsinos is required by consideration of the unification of the gauge couplings and the explanation of cosmic dark matter. It turns out that the gauge coupling unification does not necessarily require gauginos or higgsinos below the TeV scale, and they may be as heavy as 10 TeV [7,8]. However, the cosmic dark matter measured by WMAP imposes much stronger constraints on the masses of gauginos and higgsinos (except gluinos), whose lightest mass eigenstates, i.e., the lightest neutralino and chargino, must be lighter than about 1 TeV under the popular assumption $M_1 = M_2/2$, with M_1 and M_2 being the U(1) and SU(2) gaugino masses, respectively [9–12].

Note that unlike the neutralinos and charginos, the gluino is not directly subject to the dark matter constraints, and its mass, constrained by gauge coupling unification, may be as high as 18 TeV [7]. Theoretically, the gluino is usually speculated to be much heavier than neutralinos and charginos. So, although the gluino is the only colored particle among gauginos and higgsinos and is usually expected to be copiously produced in the gluon-rich environment of the LHC, it may be quite heavy and thus may be out of reach of the LHC and ILC. For studies of the split-SUSY gluino at LHC, see, e.g., [13,14]. Therefore, to explore split-SUSY, it is important to examine the neutralinos and charginos.

[a] e-mail: jmyang@itp.ac.cn

The neutralinos and charginos in split-SUSY constrained by the cosmic dark matter can be explored at the LHC and ILC in two ways. One way is directly looking for their productions, such as chargino pair productions. Our previous analysis [9] showed that the chargino pair production rates at the LHC and ILC are quite large in some part of the WMAP-allowed parameter space, but in the remaining part of the parameter space the production rates are unobservably small. The other way to reveal the existence of these particles is through disentangling their virtual effects in some processes that can be precisely measured. It has been shown that SUSY may have sizable virtual effects in Higgs boson processes (SUSY-QCD may have large residue effects in Higgs processes; see, e.g., [15–22]) and top quark processes (for SUSY-QCD effects in $t\bar{t}$ productions, see, e.g., [23–26]; for SUSY-QCD effects in FCNC top interactions, see, e.g., [27–34]), since they are the heaviest particles in the SM, and they are sensitive to new physics. For split-SUSY, its virtual effects in top quark interactions and Higgs–fermion Yukawa interactions are expected to be small, since the relevant vertex loops always involve sfermions that are superheavy. So, to reveal the virtual effects of split-SUSY, we concentrate on the gauge interactions of the Higgs boson. Such virtual effects of weakly interacting neutralinos and charginos are usually at percent level and only a high-luminosity e^+e^- collider like the ILC can possibly have such a percent-level sensitivity. As the machine for discovery, the LHC, however, is not expected to be able to disentangle such percent-level quantum effects due to its messy hadron backgrounds. So in this work we investigate the virtual effects of the WMAP-allowed split-SUSY in the Higgs productions $e^+e^- \to Zh$ and $e^+e^- \to \nu_e\bar{\nu}_e h$ through WW fusion at the ILC. Note that, although the SUSY corrections to these processes were calculated in the literature [35–37], our studies in this work are still necessary, since those calculations were performed in the framework of the general minimal supersymmetric model and did not consider the dark matter constraints.

This work is organized in the follows. In Sect. 2 we calculate the split-SUSY loop contributions to the Higgs production $e^+e^- \to Zh$ and $e^+e^- \to \nu_e\bar{\nu}_e h$ through WW fusion at the ILC. In Sect. 3 we present some numerical results for the parameter space under WMAP dark matter constraints. The conclusion is given in Sect. 4. Note that for the SUSY parameters we adopt the notation in [38, 39]. We assume that the lightest supersymmetric particle is the lightest neutralino, which solely makes up the cosmic dark matter.

2 Calculations

2.1 About split-SUSY

In split-SUSY the Higgs sector at low energy is fine-tuned to have only one Higgs doublet [4–6], and the effective spectrum of superparticles contains the higgsinos, $\tilde{H}_{u,d}$, the winos, $\tilde{W}^i$, the bino, $\tilde{B}$, and the gluino, $\tilde{g}$. The most general renormalizable Lagrangian at low energy (say the TeV scale) that contains the interactions is

$$\begin{aligned}\mathcal{L} = {} & m^2 H^\dagger H - \frac{\lambda}{2}(H^\dagger H)^2 \\ & - \Big[h^u_{ij}\bar{q}_j u_i \epsilon H^* + h^d_{ij}\bar{q}_j d_i H + h^e_{ij}\bar{\ell}_j e_i H \\ & + \frac{M_3}{2}\tilde{g}^A\tilde{g}^A + \frac{M_2}{2}\tilde{W}^a\tilde{W}^a + \frac{M_1}{2}\tilde{B}\tilde{B} \\ & + \mu\tilde{H}_u^{\mathrm{T}}\epsilon\tilde{H}_d + \frac{H^\dagger}{\sqrt{2}}\big(\tilde{g}_u\sigma^a\tilde{W}^a + \tilde{g}'_u\tilde{B}\big)\tilde{H}_u \\ & + \frac{H^{\mathrm{T}}\epsilon}{\sqrt{2}}\big(-\tilde{g}_d\sigma^a\tilde{W}^a + \tilde{g}'_d\tilde{B}\big)\tilde{H}_d + \mathrm{h.c.}\Big], \end{aligned} \tag{1}$$

where $\epsilon = \mathrm{i}\sigma_2$. Thus, the Higgs sector in split-SUSY is the same as in the SM, except for the additional Higgs couplings to the gauginos and higgsinos. The other four Higgs bosons in the MSSM are superheavy and decouple. As it is well known, an upper bound of about 135 GeV exists for the lightest Higgs boson in the MSSM [40–45], which is relaxed to about 150 GeV in split-SUSY [4–6].

The gauginos (winos and bino) and higgsinos mix into the mass eigenstates called charginos and neutralinos. The chargino mass matrix is given by

$$\begin{pmatrix} M_2 & \sqrt{2}m_W\sin\beta \\ \sqrt{2}m_W\cos\beta & \mu \end{pmatrix}, \tag{2}$$

and the neutralino mass matrix is given by

$$\begin{pmatrix} M_1 & 0 & -m_Z s_{\mathrm{W}} c_\beta & m_Z s_{\mathrm{W}} s_\beta \\ 0 & M_2 & m_Z c_{\mathrm{W}} c_\beta & -m_Z c_{\mathrm{W}} s_\beta \\ -m_Z s_{\mathrm{W}} c_\beta & m_Z c_{\mathrm{W}} c_\beta & 0 & -\mu \\ m_Z s_{\mathrm{W}} s_\beta & -m_Z c_{\mathrm{W}} s_\beta & -\mu & 0 \end{pmatrix}, \tag{3}$$

where $s_{\mathrm{W}} = \sin\theta_{\mathrm{W}}$ and $c_{\mathrm{W}} = \cos\theta_{\mathrm{W}}$, with θ_{W} being the Weinberg weak mixing angle, and $s_\beta = \sin\beta$ and $c_\beta = \cos\beta$, with β defined by $\tan\beta = v_2/v_1$, being the ratio of the vacuum expectation values of the two Higgs doublets. M_1 and M_2 are, respectively, the U(1) and SU(2) gaugino mass parameters, and μ is the mass parameter in the mixing term $-\mu\epsilon_{ij}H_u^i H_d^j$ in the superpotential. The diagonalization of (2) gives two charginos $\tilde{\chi}^+_{1,2}$ with the convention $M_{\tilde{\chi}^+_1} < M_{\tilde{\chi}^+_2}$, while the diagonalization of (3) gives four neutralinos $\tilde{\chi}^0_{1,2,3,4}$ with the convention $M_{\tilde{\chi}^0_1} < M_{\tilde{\chi}^0_2} < M_{\tilde{\chi}^0_3} < M_{\tilde{\chi}^0_4}$. So the masses and mixings of the charginos and neutralinos are determined by four parameters: M_1, M_2, μ and $\tan\beta$.

Note that the low-energy Lagrangian in (1) should be understood as an effective theory after sfermions and heavy Higgs bosons are integrated out. Then, as is discussed in [4–6], the Higgs–higgsino–gaugino couplings in (1) should deviate from the SUSY results shown in the off-diagonal elements of the mass matrices in (2) and (3), although such a deviation is numerically negligible for sufficiently heavy sfermions and heavy Higgs bosons. Since in our numerical calculations the masses of gauginos and higgsinos are below 1 TeV, while the sfermions and heavy Higgs bosons are assumed to be as heavy as 200 TeV,

the effects of these sfermions and heavy Higgs bosons in the Higgs–higgsino–gaugino couplings are very small. We checked that for the numerical results presented in the next section, the effects of these superheavy sfermions and superheavy Higgs bosons are invisibly small (the deviation of the numerical results caused by their effects is below 0.1% in magnitude).

In split-SUSY, the possible channels of Higgs (h) productions at the ILC are the Higgs-strahlung process $e^+e^- \to Z^* \to Zh$ and the WW fusion process $e^+e^- \to \nu_e\bar{\nu}_e h$. Both processes will be precisely measured at the ILC if the light Higgs boson h is indeed found at the LHC. Since these processes may be sensitive to new physics, they may serve as a good probe for TeV-scale new physics. Other channels, such as the production of h associated with a CP-odd Higgs boson A and the charged Higgs pair production, cannot occur due to the superheavy A and the superheavy charged Higgs bosons.

2.2 Split-SUSY loop effects in Higgs productions at the ILC

The tree-level $e^+e^- \to Zh$ process is shown in Fig. 1. For the one-loop effects of split-SUSY, we need to calculate the diagrams containing the effective Z-boson propagator and several effective vertices as shown in Fig. 2. Note that the box diagrams always involve sfermions in the loops and thus drop out, since all sfermions are superheavy in split-SUSY. In our calculations, we use the on-shell renormalization scheme [46]. For each effective vertex or Z-boson propagator, we need to calculate several loops plus the corresponding counterterms. For the new rare vertices induced at loop level, such as γZh, there are no corresponding counterterms. Since in split-SUSY all scalar superparticles are superheavy and decouple from this process, the loops only involve charginos and neutralinos, as shown in Fig. 3.

For the WW fusion process $e^+e^- \to \nu_e\bar{\nu}_e h$, our calculations are similar to $e^+e^- \to Zh$. The tree-level Feynman diagram is shown in Fig. 4, and for one-loop split-SUSY effects, we need to calculate the diagrams containing the effective W-boson propagator and several effective vertices, as shown in Fig. 5. Just like the diagrams shown in Fig. 3, each effective vertex or W-boson propagator contains several loops plus the corresponding counterterms, as shown in Fig. 6.

Note that for $e^+e^- \to \nu_e\bar{\nu}_e h$, in addition to the WW fusion contribution shown in Fig. 4, another contribution comes from the Higgs-strahlung process $e^+e^- \to Zh$ followed by $Z \to \nu_e\bar{\nu}_e$. The cross section of $e^+e^- \to Zh \to \nu_e\bar{\nu}_e h$ peaks at the threshold of $\sqrt{s} = M_Z + M_h$ and then falls rapidly as $\sqrt{s}$ increases, where $\sqrt{s}$ is the center-

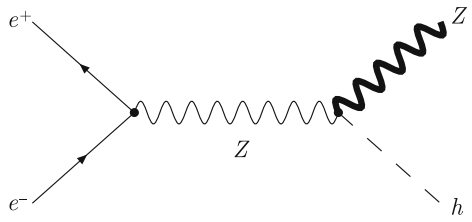

Fig. 1. Feynman diagrams for $e^+e^- \to Zh$ at tree level

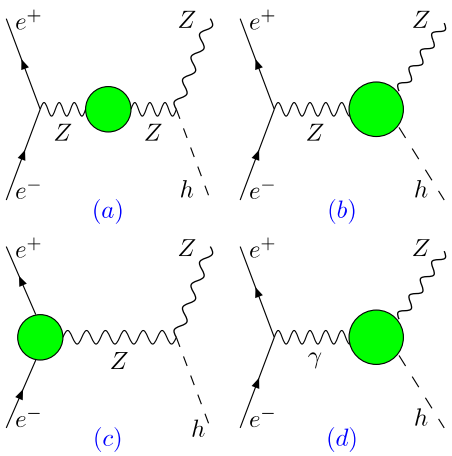

Fig. 2. Feynman diagrams for $e^+e^- \to Zh$ with one-loop corrected propagators and effective vertices in split-SUSY

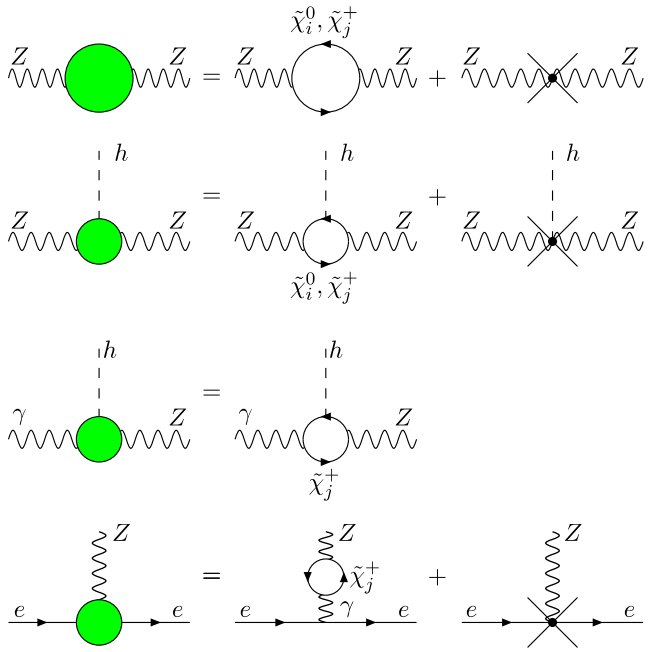

Fig. 3. Feynman diagrams for each one-loop corrected propagator and effective vertex in Fig. 2

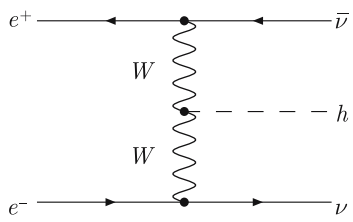

Fig. 4. Feynman diagrams for the WW fusion process $e^+e^- \to h\nu_e\bar{\nu}_e$ at tree level

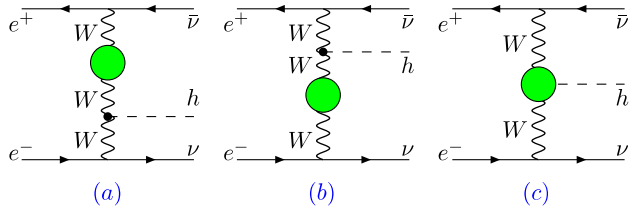

Fig. 5. Feynman diagrams for the WW fusion process $e^+e^- \to \nu_e\bar{\nu}_e h$ with one-loop corrected propogators and effective vertices

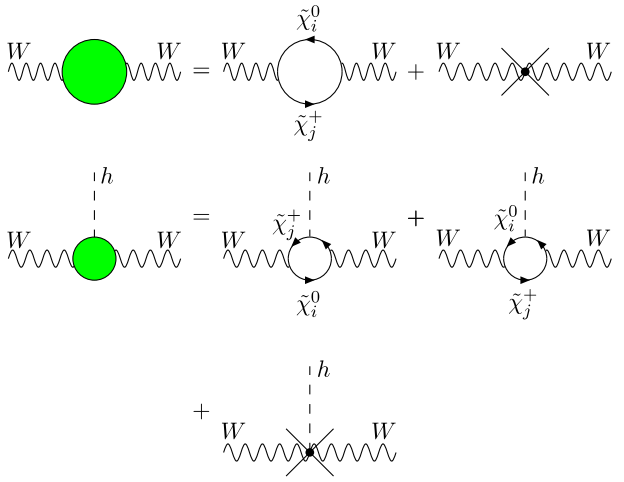

Fig. 6. Feynman diagrams for each one-loop corrected propagator and effective vertex in Fig. 5

of-mass (c.m.) energy of the e^+e^- collision. By contrast, the cross section of the WW fusion process grows monotonously as $\sqrt{s}$ increases and is by far dominant over $e^+e^- \to Zh \to \nu_e\bar{\nu}_e h$ for $\sqrt{s} \gg M_h$. In our calculation, we assume $\sqrt{s} = 1$ TeV ($\gg M_h$), and thus we only consider the WW fusion process.

Note that in the literature [36, 37] the supersymmetric corrections to this WW fusion process have been computed, but those calculations focus on the loops involving sfermions (squarks and sleptons). In our calculations in the scenario of split-SUSY, we consider the loops involving charginos and neutralinos, ignoring the loops involving sfermions, since all sfermions are superheavy in split-SUSY. So far in the literature such chargino/neutralino loop corrections have not been reported.

Each loop diagram is composed of scalar loop functions [47], which are calculated by using LoopTools [48, 49]. The calculations of the loop diagrams are tedious, and the analytical expressions are lengthy; these are not presented here.

3 Numerical results

In split-SUSY the masses of squarks and the CP-odd Higgs boson A are assumed to be arbitrarily superheavy. As our previous study showed [9], their effects in low-energy processes will decouple as long as they are heavier than about 10 TeV. The Higgs mass M_h can be calculated from Feynhiggs [50], and in our calculations we assume that the masses of squarks and Higgs boson A are 200 TeV. Among the low-energy parameters of split-SUSY, i.e., $\tan\beta$, M_2, M_1 and μ, M_h is sensitive to $\tan\beta$ and a large $\tan\beta$ leads to a large M_h. In our calculations we fix $\tan\beta = 40$, since a large value of $\tan\beta$ is favored by the current experiments. Our results are not sensitive to $\tan\beta$ in the region of a large $\tan\beta$ value, and our results are approximately valid for $\tan\beta \gtrsim 10$. With the input values of $\tan\beta$ and squark masses, we get $M_h = 120$ GeV from Feynhiggs [50].

With the value of $\tan\beta$ fixed, there remain three split-SUSY parameters: M_2, M_1 and μ. We further use the unification relation $M_1 = 5M_2 \tan^2\theta_W/3 \simeq 0.5M_2$, which is predicted in the minimal supergravity model. Thus, we finally have two free SUSY parameters. The SM parameters used in our results are taken from [51].

3.1 Numerical results without WMAP constraints

In order to show the features of our results, we first present some results without considering the WMAP dark matter constraints. In Fig. 7 we show the relative one-loop correction of split-SUSY to the cross section of $e^+e^- \to Zh$ versus the c.m. energy of the e^+e^- collision for $M_2 = 400$ GeV and $\mu = 600$ GeV. In this case the lightest chargino mass $M_{\tilde{\chi}_1^+} = 387$ GeV. We see from Fig. 7 that the corrections are negative and have a peak at $\sqrt{s} = 2M_{\tilde{\chi}_1^+}$ due to the threshold effects. The magnitude of the corrections for

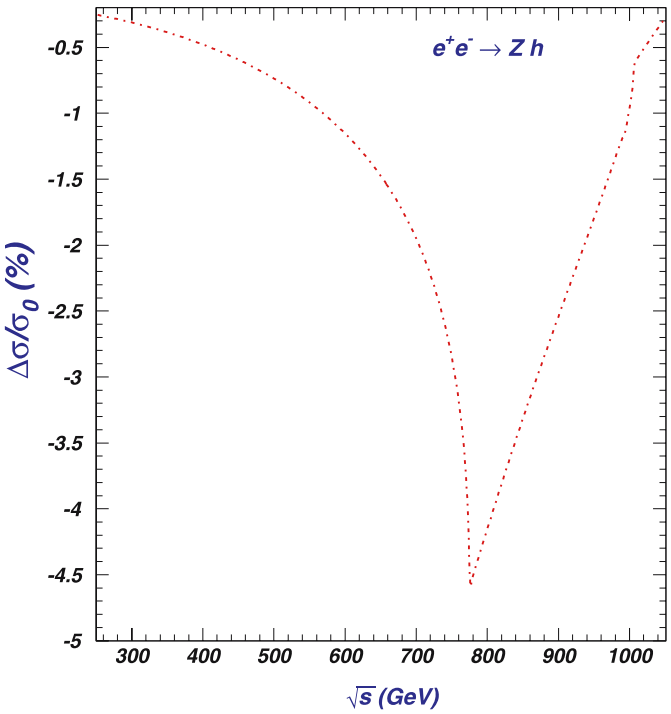

Fig. 7. The relative one-loop correction of split-SUSY to the cross section of $e^+e^- \to Zh$ versus the c.m. energy

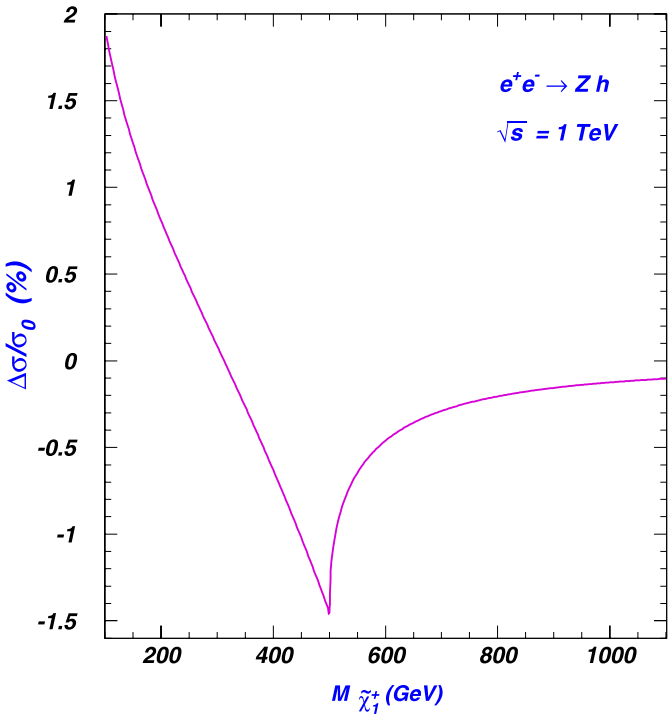

Fig. 8. Same as Fig. 7, but versus the chargino mass for a c.m. energy of 1 TeV

$\sqrt{s} = 1$ TeV, which will be taken for our following studies, is relatively small.

In Fig. 8, we fix $\sqrt{s} = 1$ TeV and $\mu = 100$ TeV (note that the scenario with a very large μ is proposed and argued for in [52]), and by varying M_2 we show the relative one-loop correction of split-SUSY to the cross section of $e^+e^- \to Zh$ versus the lightest chargino mass $M_{\tilde{\chi}_1^+}$ (in this case the chargino mass $M_{\tilde{\chi}_1^+}$ is almost equal to M_2 due to the superheavy higgsinos). The peak occurs at $M_{\tilde{\chi}_1^+} = \sqrt{s}/2$ due to threshold effects. When the chargino mass gets heavier than 1 TeV, the corrections becomes very small, showing the decoupling property.

3.2 Numerical results with WMAP constraints

Now we require that the lightest neutralinos make up the cosmic dark matter relic density measured by WMAP, which is given by $0.085 < \Omega_{\rm CDM}h^2 < 0.119$ at 2σ [53], with $h = 0.73$ being the Hubble constant. Of course, the direct bounds from LEP experiments [54] also need to be considered: (i) the lightest chargino is heavier than about 103 GeV; (ii) the lightest neutralino is heavier than about 47 GeV; (iii) the bound on the mass of the Higgs boson is $m_h > 114$ GeV (since h has almost the same interactions as in the SM).

We then perform a scan over the parameter space of M_2 and μ. The 2σ-allowed region is shown in Fig. 2 of [9]. (Note that in [9] we used the one-year WMAP data $0.094 < \Omega_{\rm CDM}h^2 < 0.129$. The allowed region with one-year WMAP data is approximately the same as that with three-year WMAP data.)

In Fig. 9, we show the one-loop correction of split-SUSY to the cross section of $e^+e^- \to Zh$ (lower panel) in comparison to the chargino pair production rate (upper panel). The chargino pair production rate is calculated at tree level, as in our previous work [9].

From Fig. 9, we see that when the chargino is lighter than about 300 GeV, the chargino pair production rate at the ILC is large, and the corresponding virtual effects in $e^+e^- \to Zh$ are positive. When the chargino gets heavier, the chargino pair production rate at the ILC drops rapidly. Of course, when the chargino is heavier than 500 GeV, beyond the threshold of the ILC (with a c.m. energy of 1 TeV), the charginos cannot be pair produced. Then it is interesting to observe that for a chargino between 500 and 600 GeV, although the ILC cannot produce chargino pairs, the virtual effects in $e^+e^- \to Zh$ can still reach a couple of percent in magnitude, and thus they may be observable at the ILC with a high integrated luminosity. Finally, when the chargino is heavier than about 600 GeV, it will probably remain inaccessible, because both the chargino pair production rates and the virtual effects are very small due to the decoupling property of SUSY.

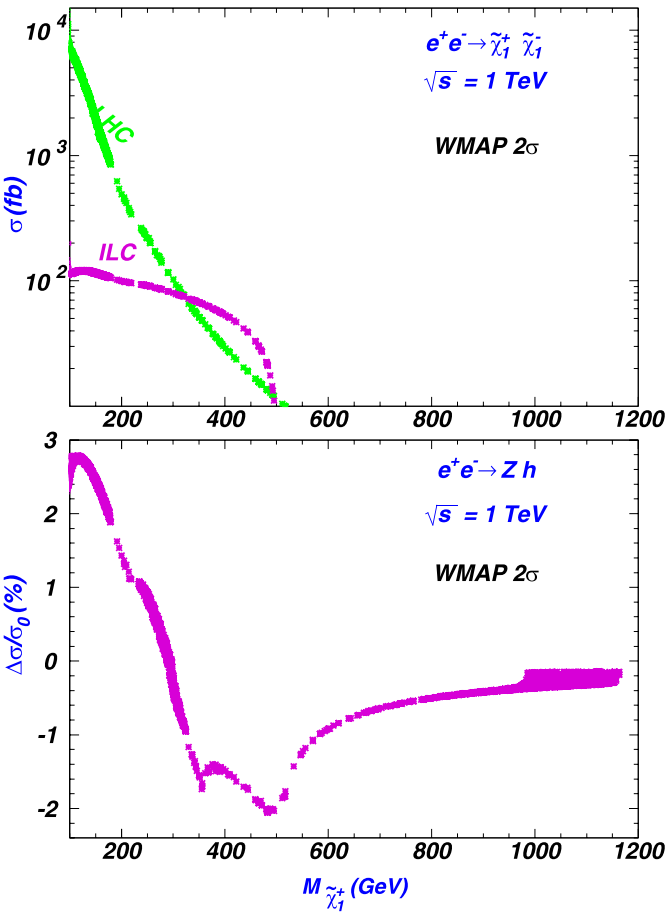

Fig. 9. The *shaded areas* are the 2σ region of split-SUSY parameter space allowed by the WMAP dark matter measurement in the planes of the chargino pair production rate (*upper panel*) and the one-loop correction of split-SUSY to the cross section of $e^+e^- \to Zh$ (*lower panel*) versus the chargino mass

Note that for $e^+e^- \to Zh$ we numerically compared our results with the full one-loop corrections given in [35] (we thank the authors of [35] for giving us their fortran code). In our calculations we only considered the chargino and neutralino loops, while in their calculations the sfermion loops are also considered besides the chargino and neutralino loops. In principle, their results in the limit of superheavy sfermions should approach our results. We found that, although their fortran code does not work well for superheavy sfermions (say above 10 TeV) due to the limitation of the numerical calculation, for a given point in the parameter space our results agree well with those by using their fortran code with all sfermions above 1 TeV.

The one-loop correction of split-SUSY to the cross section of the WW fusion process $e^+e^- \to \nu_e\bar{\nu}_e h$ is very small in magnitude, below one percent, as shown in Fig. 10. Even with a high luminosity the ILC can hardly reveal such a small deviation from the measurement of this process. The reason why the virtual effects in the s-channel process $e^+e^- \to Zh$ are much larger in magnitude than in the t-channel process $e^+e^- \to \nu_e\bar{\nu}_e h$ may be that, for the s-channel process, the virtual sparticles (charginos and neutralinos) in the loops could be more energetic and cause larger quantum effects.

Anyway, such virtual effects of split-SUSY, no matter if they are large or small in magnitude, could be informative and complementary to the real sparticle productions in probing split-SUSY at colliders. For example, if split-SUSY turns out to be the true story, and the chargino pair production is observed with the chargino mass around 150 GeV at the ILC, then we know from Figs. 9 and 10 that the virtual effects of SUSY must be about 2.5% for the process $e^+e^- \to Zh$ and -0.1% for the WW fusion process $e^+e^- \to \nu_e\bar{\nu}_e h$.

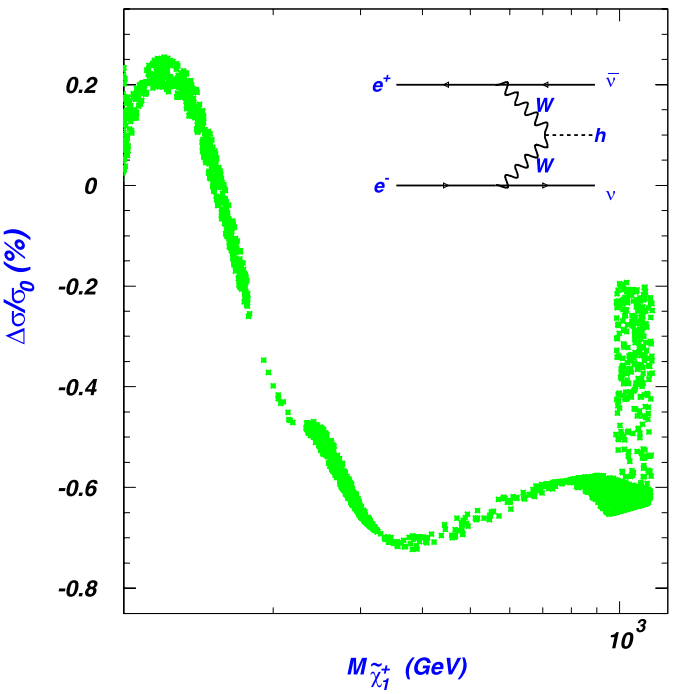

Fig. 10. Same as the lower panel of Fig. 9, but for the WW fusion process $e^+e^- \to \nu_e\bar{\nu}_e h$

4 Conclusion

In split supersymmetry, gauginos and higgsinos are the only supersymmetric particles possibly accessible at foreseeable colliders like the LHC and the ILC. In order to account for the cosmic dark matter measured by WMAP, the parameter space of the gauginos and higgsinos in split supersymmetry is stringently constrained, which can be explored at the LHC and the ILC through direct productions and the virtual effects of these gauginos and higgsinos. The clean environment of the ILC may render the virtual effects at percent level meaningful in probing new physics. In this work, we assumed split supersymmetry and calculated the virtual effects of the WMAP-allowed gauginos and higgsinos in the Higgs productions $e^+e^- \to Zh$ and $e^+e^- \to \nu_e\bar{\nu}_e h$ through WW fusion at the ILC. We found that the production cross section of $e^+e^- \to Zh$ can be altered by a few percent in some part of the WMAP-allowed parameter space, while the correction to the WW fusion process $e^+e^- \to \nu_e\bar{\nu}_e h$ is below 1%.

Such virtual effects are correlated with the cross sections of chargino pair productions and thus can offer complementary information in probing split supersymmetry at the colliders. Our results indicate that if the lightest chargino is in the light region allowed by the WMAP dark matter (say below 200 GeV), then at the ILC and LHC the chargino pair production rates are large, and the virtual effects of charginos/neutralinos in the process $e^+e^- \to Zh$ at the ILC can reach a few percent; both may be measurable and may be cross-checked. An interesting observation is that for a chargino between 500 and 600 GeV, although the ILC (with c.m. energy of 1 TeV) cannot produce chargino pairs, the virtual effects in $e^+e^- \to Zh$ can still reach a couple of percent in magnitude and thus may be observable at the ILC with a high integrated luminosity. The WMAP-allowed region with the chargino heavier than about 600 GeV will most likely remain inaccessible, because both the chargino production rates and the virtual effects are very small due to the decoupling property of SUSY.

Acknowledgements. This work is supported in part by the National Natural Science Foundation of China.

References

1. K. Abe et al., hep-ph/0109166
2. T. Abe et al., hep-ex/0106056
3. J.A. Aguilar-Saavedra et al., hep-ph/0106315
4. N. Arkani-Hamed, S. Dimopoulos, hep-th/0405159
5. G.F. Giudice, A. Romanino, Nucl. Phys. B **699**, 65 (2004)
6. N. Arkani-Hamed, S. Dimopoulos, G.F. Giudice, A. Romanino, Nucl. Phys. B **709**, 3 (2005)
7. L. Senatore, Phys. Rev. D **71**, 103 510 (2005)

8. F. Wang, W.Y. Wang, J.M. Yang, Phys. Rev. D **72**, 077 701 (2005)
9. F. Wang, W.Y. Wang, J.M. Yang, Eur. Phys. J. C **46**, 521 (2006)
10. A. Pierce, Phys. Rev. D **70**, 075 006 (2004)
11. A. Arvanitaki, P.W. Graham, hep-ph/0411376
12. A. Masiero, S. Profumo, P. Ullio, Nucl. Phys. B **712**, 86 (2005)
13. K. Cheung, W.-Y. Keung, Phys. Rev. D **71**, 015 015 (2005)
14. J.G. Gonzalez, S. Reucroft, J. Swain, Phys. Rev. D **74**, 027 701 (2006)
15. G. Gao, R.J. Oakes, J.M. Yang, Phys. Rev. D **71**, 095 005 (2005)
16. J. Cao et al., Phys. Rev. D **68**, 075 012 (2003)
17. G. Gao et al., Phys. Rev. D **66**, 015 007 (2002)
18. H.E. Haber et al., Phys. Rev. D **63**, 055 004 (2001)
19. M.J. Herrero, S. Peñaranda, D. Temes, Phys. Rev. D **64**, 115 003 (2001)
20. A. Dobado, M.J. Herrero, Phys. Rev. D **65**, 075 023 (2002)
21. M. Carena et al., Phys. Rev. D **60**, 075 010 (1999)
22. M. Carena et al., Phys. Rev. D **62**, 055 008 (2000)
23. C.S. Li et al., Phys. Rev. D **52**, 5014 (1995)
24. C.S. Li et al., Phys. Lett. B **379**, 135 (1996)
25. S. Alam, K. Hagiwara, S. Matsumoto, Phys. Rev. D **55**, 1307 (1997)
26. Z. Sullivan, Phys. Rev. D **56**, 451 (1997)
27. C.S. Li, R.J. Oakes, J.M. Yang, Phys. Rev. D **49**, 293 (1994)
28. G. Couture, C. Hamzaoui, H. Konig, Phys. Rev. D **52**, 1713 (1995)
29. J.L. Lopez, D.V. Nanopoulos, R. Rangarajan, Phys. Rev. D **56**, 3100 (1997)
30. G.M. de Divitiis, R. Petronzio, L. Silvestrini, Nucl. Phys. B **504**, 45 (1997)
31. C.S. Li et al., Phys. Lett. B **599**, 92 (2004)
32. J. Cao et al., Nucl. Phys. B **651**, 87 (2003)
33. J. Cao et al., Phys. Rev. D **74**, 031 701 (2006)
34. M. Frank, I. Turan, Phys. Rev. D **74**, 073 014 (2006)
35. P. Chankowski, S. Pokorski, J. Rosiek, Nucl. Phys. B **423**, 437 (1994)
36. T. Hahn et al., Nucl. Phys. B **652**, 229 (2003)
37. H. Eberl et al., Nucl. Phys. B **657**, 378 (2003)
38. H.E. Haber, G.L. Kane, Phys. Rep. **117**, 75 (1985)
39. J.F. Gunion, H.E. Haber, Nucl. Phys. B **272**, 1 (1986)
40. H.E. Haber, R. Hempfling, Phys. Rev. Lett. **66**, 1815 (1991)
41. Y. Okada, M. Yamaguchi, T. Yanagida, Prog. Theor. Phys. **85**, 1 (1991)
42. Y. Okada, M. Yamaguchi, T. Yanagida, Phys. Lett. B **262**, 54 (1991)
43. J. Ellis, G. Ridolfi, F. Zwirner, Phys. Lett. B **257**, 83 (1991)
44. J. Ellis, G. Ridolfi, F. Zwirner, Phys. Lett. B **262**, 477 (1991)
45. J.R. Espinosa, R.J. Zhang, JHEP **0003**, 026 (2000)
46. A. Denner, Fortschr. Phys. **41**, 4 (1993)
47. G. 't Hooft, M.J.G. Veltman, Nucl. Phys. B **153**, 365 (1979)
48. T. Hahn, M. Perez-Victoria, Comput. Phys. Commun. **118**, 153 (1999)
49. T. Hahn, Nucl. Phys. Proc. Suppl. **135**, 333 (2004)
50. S. Heinemeyer, hep-ph/0407244
51. W.M. Yao et al., J. Phys. G **33**, 1 (2006)
52. K. Cheung, C.-W. Chiang, Phys. Rev. D **71**, 095 003 (2005)
53. D.N. Spergel et al., astro-ph/0603449
54. LEP2 SUSY Working Group homepage, http://lepsusy.web.cern.ch/lepsusy/